

## Observation of Out-of-Phase Bilayer Plasmons in $\text{YBa}_2\text{Cu}_3\text{O}_{7-\delta}$

M. Grüninger,<sup>1,\*</sup> D. van der Marel,<sup>1</sup> A. A. Tsvetkov,<sup>1,†</sup> and A. Erb<sup>2</sup>

<sup>1</sup>Laboratory of Solid State Physics, MSC, University of Groningen, Nijenborgh 4, 9747 AG Groningen, The Netherlands

<sup>2</sup>Département de Physique de la Matière Condensée, University of Geneva, CH-1211 Geneva 4, Switzerland

(Received 16 March 1999)

The temperature dependence of the  $c$ -axis optical conductivity  $\sigma(\omega)$  of optimally and overdoped  $\text{YBa}_2\text{Cu}_3\text{O}_x$  ( $x = 6.93$  and  $7$ ) is reported in the far- (FIR) and midinfrared (MIR) range. Below  $T_c$  we observe a transfer of spectral weight from the FIR not only to the condensate at  $\omega = 0$ , but also to a new peak in the MIR. This peak is naturally explained as a transverse out-of-phase bilayer plasmon by a model for  $\sigma(\omega)$  which takes the layered crystal structure into account. With decreasing doping the plasmon shifts to lower frequencies and can be identified with the surprising and so far not understood FIR feature reported in *underdoped* bilayer cuprates.

PACS numbers: 74.25.Gz, 71.45.Gm, 74.72.Bk

After many years, the discussion about the charge dynamics perpendicular to the  $\text{CuO}_2$  layers of the high  $T_c$  cuprates is still very controversial. The role attributed to interlayer hopping ranges from negligible to being the very origin of high  $T_c$  superconductivity [1]. There is no agreement about the relevant excitations nor about the dominant scattering mechanism. The  $c$ -axis resistivity  $\rho_c$  is much larger than predicted by band structure calculations. The anisotropy  $\rho_c/\rho_{ab}$  can be as large as  $10^5$  and shows a strong temperature dependence, especially in the underdoped regime, which has been interpreted as an indication for non-Fermi liquid behavior and confinement [2]. This strong temperature dependence is due to two different regimes with  $d\rho_c/dT < 0$  for  $T_c < T < T'$  and  $d\rho_c/dT > 0$  for  $T > T'$ , with a crossover temperature  $T'$  that decreases with increasing doping. There is some agreement as to the phenomenology that  $\rho_c$  is described by a *series* of resistors [2–4], i.e., that different contributions have to be added, and that the sign change in  $d\rho_c/dT$  is due to the different temperature dependence of the competing contributions. Overdoped  $\text{YBa}_2\text{Cu}_3\text{O}_x$  (YBCO) is often regarded as a remarkable exception, as  $\rho_c/\rho_{ab}$  is only about 50, and  $d\rho_c/dT > 0$  for all  $T > T_c$ . It is an important issue whether a sign change in  $d\rho_c/dT$  at low  $T$  is really absent or only hidden by  $T_c$  being larger than a possible  $T'$ , i.e., whether overdoped YBCO follows anisotropic three dimensional (3D) or rather 2D behavior.

The  $c$ -axis optical conductivity  $\sigma_1(\omega)$  of YBCO shows several remarkable features [5–9]: (1) a very low value compared to band structure calculations, reflecting the large  $\rho_c$ ; (2) a suppression of spectral weight at low frequencies already above  $T_c$  in underdoped samples referred to as the opening of a “pseudogap” (which agrees with the upturn in  $\rho_c$ ); (3) the appearance of an intriguing broad “bump” in the far infrared (FIR) at low  $T$  in underdoped samples; (4) in overdoped YBCO, the spectral weight of the superconducting condensate is overestimated from  $\sigma_1(\omega)$  as compared to microwave techniques [10].

In this Letter, we suggest that most of the above mentioned issues can be clarified by modeling the cuprates, or

in particular YBCO as a stack of coupled  $\text{CuO}_2$  layers with alternating weaker and stronger links, extending on an earlier publication [11], where a *transverse* optical plasmon was predicted in Josephson coupled bilayer cuprates. This model has been verified in  $\text{SmLa}_{0.8}\text{Sr}_{0.2}\text{CuO}_{4-\delta}$  [12]. We report the observation of the transverse mode in the infrared spectrum of optimally and overdoped YBCO and propose a common origin with the above mentioned bump in underdoped YBCO. The multilayer model fits the measured data at all doping levels and at all temperatures. Our observations can be regarded as a realization of the “excitons” first considered by Leggett [13], which involve the relative phase fluctuations of the condensates formed in two different bands crossing the Fermi surface.

Single crystals of  $\text{YBa}_2\text{Cu}_3\text{O}_x$  were grown using the recently developed  $\text{BaZrO}_3$  crucibles [14], which in contrast to other container materials do not pollute the resulting crystals. Crystals grown using this technique exhibit therefore a superior purity ( $>99.995$  at. %) [15]. The samples had typical dimensions of  $2 \times (0.5-0.7)$  mm<sup>2</sup> in the  $ac$  plane. The O concentration was fixed by annealing according to the calibration of Lindemer [16]. An O content of  $x = 7$  was obtained by annealing for 400 h at 300 °C in 100 bar of high purity oxygen. Annealing in flowing oxygen at 517 °C for 260 h produced  $x = 6.93$ . Measurements of the ac susceptibility indicate  $T_c = 91$  K for  $x = 6.93$  and 87 K for  $x = 7$ . The widths of the transitions were 0.2 and 1 K, respectively. Polarized reflection measurements were carried out on a Fourier transform spectrometer between 50 and 3000 cm<sup>-1</sup> for temperatures between 4 and 300 K. As a reference we used an *in situ* evaporated Au film. Above 2000 cm<sup>-1</sup> the spectra are almost  $T$  independent. The optical conductivity  $\sigma(\omega)$  was calculated via a Kramers-Kronig analysis.

The measured  $c$ -axis reflectivity and  $\sigma_1(\omega)$  derived from it are plotted in Fig. 1 for 4 and 100 K (solid and dashed black lines). Disregarding the phonons,  $\sigma_1(\omega)$  shows an almost constant value of about  $200 \Omega^{-1} \text{cm}^{-1}$  above  $T_c$ ; a Drude-like upturn is observed only at low frequencies in the overdoped case  $x = 7$ . Below  $T_c$

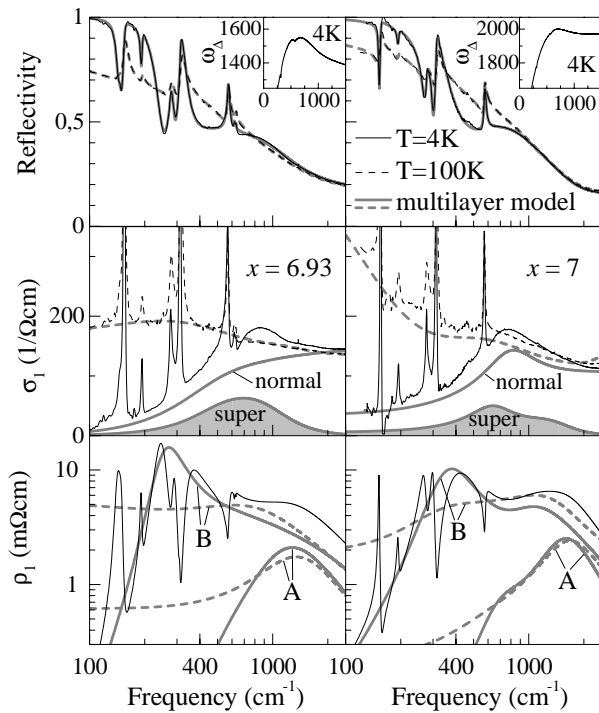


FIG. 1. The  $c$ -axis reflectivity  $R$ ,  $\text{Re}\sigma(\omega)$  and  $\text{Re}\rho(\omega)$  above (dashed lines) and below  $T_c$  (solid lines) for  $x = 6.93$  (left panels) and  $x = 7$  (right). The thick gray lines depict fits of  $R$  using the multilayer model and, in  $\text{Re}\sigma(\omega)$ , the normal carrier electronic contribution  $\sigma_{en}(\omega)$  derived from it. The filled areas show  $\sigma_{es}(\omega)$  as defined in the text. In order to demonstrate that the total  $\text{Re}\rho(\omega)$  is a linear superposition of the subcell contributions, we display the electronic contributions  $\text{Re}\rho_A$  and  $\text{Re}\rho_B$  along with the total dynamical resistivity including the phonons, as obtained from the fit in the upper panel. Insets:  $\omega_{\Delta}(4\text{ K}, \omega)$  as defined in Eq. (1).

a sharp reflectivity edge develops at about  $300\text{ cm}^{-1}$ , which had been identified as a Josephson plasmon, a collective mode in a stack of Josephson coupled 2D superconducting layers. The gradual suppression of  $\sigma_1(\omega)$  below about  $700\text{ cm}^{-1}$  can be attributed to the opening of the superconducting gap. The observation of excess conductivity between  $700$  and  $1500\text{ cm}^{-1}$  below  $T_c$  is a central issue in the present discussion. The superconducting phase transition obeys case II coherence factors for electromagnetic absorption [17]. As a result in the dirty limit, relevant for  $c$ -axis transport, only a *suppression* of  $\sigma_1(\omega)$  is expected for frequencies not too close to 0. The difference of spectral weight above and below  $T_c$  defined as (for  $T < T_c$ ):

$$\omega_{\Delta}^2(T, \omega) = 8 \int_{0^+}^{\omega} [\sigma_1(100\text{ K}, \omega') - \sigma_1(T, \omega')] d\omega' \quad (1)$$

is expected to rise monotonically with increasing frequency to a constant value for frequencies much larger than the gap. Our data clearly indicate a nonmonotonic

behavior of  $\omega_{\Delta}(\omega)$  (insets in Fig. 1; see also Ref. [7]) and a spectral weight transfer from low frequencies to a new peak above the phonons; i.e., opposite to the trend observed in some of the other cuprates [18]. This can be naturally explained by the following model for  $\sigma(\omega)$  which takes into account the layered structure of the cuprates.

We divide the unit cell of YBCO into the intra- and interbilayer subcells  $A$  and  $B$ . Let us imagine that a time dependent current is induced along the  $c$  direction, the time derivative of which is  $(dJ_c/dt)$ . We define  $(dV_j/dt)$  as the time derivative of the voltage between two neighboring  $\text{CuO}_2$  layers, i.e., across subcell  $j$ . Our multilayer model corresponds to the approximation, that the ratio  $(dV_j/dt)/(dJ_c/dt)$  is provided by a *local* linear response function  $\rho_j$  corresponding to the complex impedance which depends *only* on the voltage variations on the neighboring  $\text{CuO}_2$  layers, and not on the voltages on layers further away. Microscopically this corresponds to the condition, that in the normal state the mean free path along  $c$  must be shorter than the distance between the layers,  $l_j$ . In the superconducting state this should be supplemented with the same condition for the coherence length along  $c$ . In this sense, the multilayer model reflects the confinement of carriers in individual 2D  $\text{CuO}_2$  layers. Let us treat the current as the parameter controlled by applying an external field. Since the current between the layers is now uniform and is independent of the subcell index  $j$ , the electric field average over the unit cell is a linear superposition of the voltages over all subcells within the unit cell. This effectively corresponds to putting the complex impedances  $\rho_j$  of subcells *in series*,  $\rho(\omega) = x_A \rho_A(\omega) + x_B \rho_B(\omega)$ , where the  $x_j = l_j/l_c$  are the relative volume fractions of the two subcells,  $l_A + l_B = l_c$ , and  $\rho_j(\omega)$  are the *local* impedance functions within subcells  $A$  and  $B$ . This sum for  $\rho(\omega) = [\sigma(\omega) + \omega/4\pi i]^{-1}$  is very different from the case of a homogeneous medium, where different contributions are additive in  $\sigma(\omega) = \sum \sigma_j(\omega)$ , which corresponds to putting the various conducting channels of the medium *in parallel*. To illustrate this, let us adopt the Drude model for the complex interlayer impedance. In parallel conduction the sum of, e.g., two Drude peaks yields

$$\frac{4\pi i/\omega}{\rho(\omega)} = 1 - \frac{\omega_{p,A}^2}{\omega^2 + i\gamma_A\omega} - \frac{\omega_{p,B}^2}{\omega^2 + i\gamma_B\omega}, \quad (2)$$

where  $\omega_{p,j}$  denotes the plasma frequency, and  $\gamma_j$  labels the damping. This results in a single plasma resonance at a frequency  $\omega_p^2 = \omega_{p,A}^2 + \omega_{p,B}^2$ , i.e., only one longitudinal mode (the zero) survives which is shifted with respect to the zeros of the individual components. The transverse mode (the pole at  $\omega = 0$ ) is identical. Putting two Drude oscillators *in series* in the multilayer model, i.e., using  $\sum x_j \rho_j$ , has a surprising consequence.

$$\frac{\rho(\omega)}{4\pi i/\omega} = \frac{x_A}{1 - \frac{\omega_{p,A}^2}{\omega^2 + i\gamma_A\omega}} + \frac{x_B}{1 - \frac{\omega_{p,B}^2}{\omega^2 + i\gamma_B\omega}}. \quad (3)$$

Now both longitudinal modes (poles of  $\rho_j$ ) are unaffected, and in between a new *transverse* mode arises at  $\omega_0 = (x_A\omega_{p,B}^2 + x_B\omega_{p,A}^2)^{1/2}$  (for zero damping). This transverse optical plasmon can be regarded as an out-of-phase oscillation of the two individual components. This mode has been predicted in Ref. [11] for the case of a multilayer of Josephson coupled 2D superconducting layers. The existence of two longitudinal modes was confirmed experimentally in  $\text{SmLa}_{0.8}\text{Sr}_{0.2}\text{CuO}_{4-\delta}$  [12]. Note that superconductivity is not a necessary ingredient; the optical plasmon appears regardless of the damping of the individual components.

In order to apply the model to the measured reflectivity data, we have to include the phonons, for which a separation into subcells is not generally justified, e.g., for the *c*-axis bending mode of the planar O ions, located on the border between subcells *A* and *B*. Therefore we adopt the following model impedance:

$$\rho(\omega) = \sum_j \frac{x_j}{\sigma_j + \sigma_{ph} + \sigma_M + \omega/4\pi i}, \quad j \in \{A, B\}, \quad (4)$$

where  $x_A = 0.28$ , and  $x_B = 1 - x_A$  for YBCO. Note that this model reduces to the conventional expression for a homogeneous medium commonly used for high  $T_c$  superconductors if we either set  $x_A = 0$  or  $\sigma_A = \sigma_B$ . The  $\sigma_{A,B}(\omega)$  contain the purely electronic contributions with eigenfrequency  $\omega_0 = 0$  within each subcell.

$$4\pi\sigma_j(\omega) = \frac{i\omega_{s,j}^2}{\omega} + \frac{i\omega_{n,j}^2}{\omega + i\gamma_j}, \quad j \in \{A, B\}, \quad (5)$$

where  $\omega_{s,j}$  and  $\omega_{n,j}$  label the plasma frequencies of superconducting and normal carriers, respectively. All other contributions [phonons, midinfrared (MIR) oscillators, etc.] are assumed to be identical in the two subcells and are included in a sum of Lorentz oscillators

$$\frac{4\pi i}{\omega} [\sigma_{ph} + \sigma_M] = \sum \frac{\omega_{p,j}^2}{\omega_{0,j}^2 - \omega^2 - i\gamma_j\omega}, \quad (6)$$

where  $\omega_{0,j}$  denotes the *j*th peak frequency.

The parameters used in the fit are given in Table I. In the superconducting state the electronic response is described with nine adjustable parameters (including a broad mid-infrared band). The same number of parameters is used in a conventional multioscillator fit with  $\omega_n$  and  $\gamma$  of a Drude term,  $\omega_s$  of a London term, a Lorentz oscillator for the ‘‘bump,’’ and a broad midinfrared oscillator. The agreement between the measured reflectivity data and fits using this model is very good at all temperatures (thick gray lines in Fig. 1). The strong MIR peak of the optical plasmon caused by the out-of-phase oscillation of the superconducting carriers in the two subcells is very well

TABLE I. Parameters  $\omega_s$ ,  $\omega_n$ ,  $\omega_0$ ,  $\omega_p$  and  $\gamma$  in units of  $\text{cm}^{-1}$  used for fitting the infrared reflectivities. The labels *A* (intra-bilayer), *B* (interbilayer), and *M* refer to Eq. (4).

$x = 7.0$		$x = 6.93$	
4 K	100 K	4 K	100 K
<i>A</i> , electronic ( $\omega_s, \omega_n, \gamma$ ):			
3461, 1182, 600	0, 3389, 150	3480, 0, 0	0, 3677, 498
<i>B</i> , electronic ( $\omega_s, \omega_n, \gamma$ ):			
1526, 1171, 700	0, 1814, 142	1311, 0, 0	0, 2146, 563
<i>M</i> , electronic ( $\omega_0, \omega_p, \gamma$ ):			
796, 1511, 633	629, 2837, 1343	525, 1131, 762	906, 3818, 4078
Phonons ( $\omega_0, \omega_p, \gamma$ ):			
155, 272, 1.2	154, 301, 2.0	155, 338, 2.4	155, 396, 3.4
194, 121, 4.3	195, 109, 5.0	193, 133, 4.0	194, 113, 5.2
278, 256, 13	280, 300, 22	279, 271, 13	280, 272, 13
312, 382, 4.3	315, 372, 7.4	313, 453, 4.6	316, 526, 10
573, 333, 9.2	573, 315, 12	568, 428, 12	569, 403, 16
		618, 92, 7.3	618, 116, 10
		630, 56, 4.2	630, 77, 6.0

reproduced. In the bottom panels of Fig. 1 we plot the real part of the dynamical resistivity  $\rho(\omega)$ . The thin black line was obtained from the full fit parameters and agrees with the Kramers-Kronig result. The electronic contribution  $\rho_e(\omega)$  was obtained by leaving out the phonon part  $\sigma_{ph}(\omega)$  from the fit parameters in Eq. (4). In the multilayer model  $\rho_e(\omega)$  is the sum of the subcell contributions  $x_j\rho_{ej} = x_j/(\sigma_j + \sigma_M + \omega/4\pi i)$  ( $j \in \{A, B\}$ , solid gray lines), which shows that  $\rho(\omega)$  is a linear superposition of the two plasmon peaks in the two subcells. Contrary to the conventional model, the different contributions are not strictly additive in  $\sigma_1(\omega)$  due to the inverse summation in Eq. (4). Nevertheless, we can calculate an estimate of the electronic contribution  $\sigma_e(\omega)$  from the fit parameters in the same way as done for  $\rho_e$ . An estimate of only the normal electronic contribution  $\sigma_{en}(\omega)$  is obtained by leaving out the London terms  $\propto \omega_{s,j}^2$  together with  $\sigma_{ph}$ . The contribution arising from the presence of superconducting carriers is then defined as  $\sigma_{es}(\omega) = \sigma_e(\omega) - \sigma_{en}(\omega)$  (see Fig. 1).

With decreasing doping level the absolute value of  $\sigma_1(\omega)$  decreases and therefore the optical plasmon peak becomes sharper. At the same time, all plasma frequencies and hence also the optical plasma mode shift to lower frequencies. This scenario explains the strong FIR bump reported in underdoped YBCO [5,6]. Similar bumps have been observed in other bilayer cuprates [19,20], but never in a single layer material. This bump has hindered an unambiguous separation of electronic and phononic contributions to  $\sigma_1(\omega)$ . In Fig. 2 we show reflectivity spectra of underdoped samples of YBCO taken from Refs. [5,6] together with fits using the multilayer model. Again good agreement with the model is obtained. Previously it was argued that the phonon spectral weight is only conserved

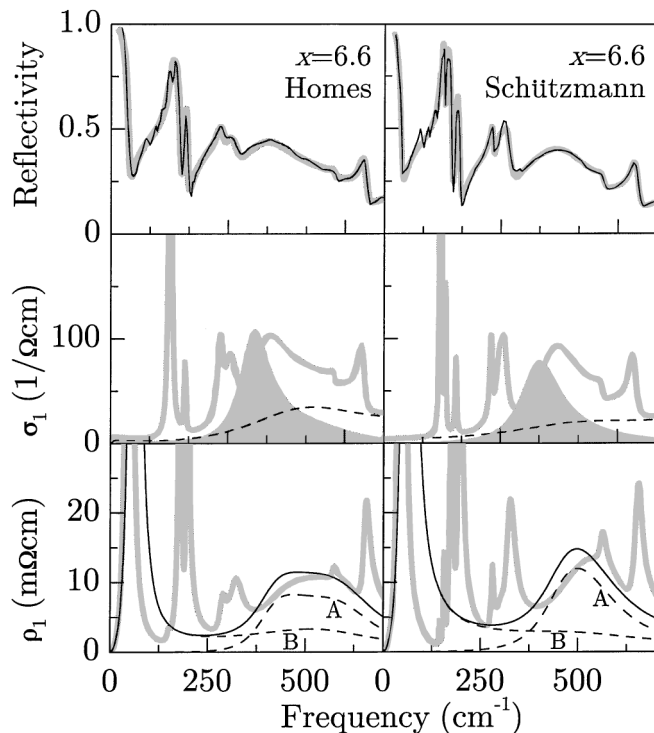


FIG. 2. Reflectivity data at 4 K from Refs. [5,6] and fits using the multilayer model. In all panels the thick gray lines show the fit result. The mid panels show  $\sigma_1(\omega)$  and the different electronic contributions to it [ $\sigma_{es}(\omega)$ : filled area,  $\sigma_{en}(\omega)$ : dashed line]. The solid lines in the bottom panels show the electronic contributions to  $\rho(\omega)$  and the separation into subcells A and B (dashed lines). Intra- and interbilayer Josephson plasma frequencies  $\omega_{s,j}$  of 1574 and 199  $\text{cm}^{-1}$  (left panels) and of 1449 and 187  $\text{cm}^{-1}$  (right) were used in the fit.

for different  $T$  if the bump is interpreted as a phonon [5]. However, a sum rule exists only for the total  $\sigma_1(\omega)$ , not for the phonon part separately. Moreover, in this scenario the width of the bump, its temperature and doping dependence, and the phonon asymmetries remained unexplained. Munzar *et al.* [21] recently showed that the phonon anomalies can be naturally explained by changes of the local fields acting on the ions arising from the onset of inter- and intrabilayer Josephson effects.

Both the low frequency Josephson plasmon and the bump are suppressed simultaneously by Zn substitution [8], which supports our assignment that both peaks are plasma modes. An increase of spectral weight of the bump with decreasing  $T$  was reported to start far above  $T_c$  [5,6], but a distinct peak is observed only below  $T_c$ . We obtained good fits for all  $T$  (not shown). As mentioned above, superconductivity is not a necessary ingredient of the multilayer model—an out-of-phase motion of normal carriers will give rise to a peak at finite frequencies, too. Upon cooling below  $T_c$ , the reduction of the underlying electronic conductivity due to the opening of a gap and the reduced damping of the plasmon produce a distinct peak.

Our results imply that the  $c$ -axis transport of *quasiparticles* is incoherent even between the two layers of a bilayer, which agrees with the absence of a bilayer bonding-antibonding (BA) transition in our spectra. Using photoelectron spectroscopy [22] a BA splitting of about 3000  $\text{cm}^{-1}$  was reported. The anomalous broad photoemission line shape may explain the absence thereof in the optical data.

In conclusion, we observed the out-of-phase bilayer plasmon predicted by the multilayer model. The good agreement of the optical data with the multilayer model at all temperatures and doping levels shows that YBCO can be modeled by local electrodynamics along the  $c$  axis in both the normal and the superconducting state. Our results strongly point towards a non-Fermi-liquid picture and confinement of carriers to single  $\text{CuO}_2$  layers.

We gratefully acknowledge C. Bernhard and S. Tajima for helpful discussions. The project is supported by the Netherlands Foundation for Fundamental Research on Matter (FOM) with financial aid from the Nederlandse Organisatie voor Wetenschappelijk Onderzoek (NWO).

\*Present address: II. Physical Institute, University of Cologne, Germany.

†Also at P.N. Lebedev Physical Institute, Moscow, Russia.

- [1] For a review, see S.L. Cooper and K.E. Gray, in *Physical Properties of High Temperature Superconductors IV*, edited by D.M. Ginsberg (World Scientific, Singapore, 1994).
- [2] P.W. Anderson, *The Theory of Superconductivity in the High- $T_c$  Cuprates* (Princeton University Press, Princeton, New Jersey, 1997).
- [3] Y.F. Yan *et al.*, Phys. Rev. B **52**, R751 (1995).
- [4] I. Terasaki *et al.*, Phys. Rev. B **52**, 16 246 (1995).
- [5] C.C. Homes *et al.*, Can. J. Phys. **73**, 663 (1995).
- [6] J. Schützmann *et al.*, Phys. Rev. B **52**, 13 665 (1995).
- [7] S. Tajima *et al.*, Phys. Rev. B **55**, 6051 (1997).
- [8] R. Hauff *et al.*, Phys. Rev. Lett. **77**, 4620 (1996).
- [9] C. Bernhard *et al.*, Phys. Rev. Lett. **80**, 1762 (1998).
- [10] C.C. Homes *et al.*, Physica (Amsterdam) **296C**, 230 (1998).
- [11] D. van der Marel and A. Tsvetkov, Czech. J. Phys. **46**, 3165 (1996).
- [12] H. Shibata and T. Yamada, Phys. Rev. Lett. **81**, 3519 (1998).
- [13] A.J. Leggett, Prog. Theor. Phys. **36**, 901 (1966).
- [14] A. Erb, E. Walker, and R. Flükiger, Physica (Amsterdam) **245C**, 245 (1995); **258C**, 9 (1996).
- [15] A. Erb *et al.*, Physica (Amsterdam) **282C–287C**, 89 (1997); **282C–287C**, 459 (1997).
- [16] T.B. Lindemer *et al.*, J. Am. Ceram. Soc. **72**, 1775 (1989).
- [17] M. Tinkham, *Introduction to Superconductivity* (McGraw-Hill, New York, 1983), 2nd ed.
- [18] D.N. Basov *et al.*, Science **283**, 49 (1999).
- [19] M. Reedyk *et al.*, Phys. Rev. B **49**, 15 984 (1994).
- [20] D.N. Basov *et al.*, Phys. Rev. B **50**, 3511 (1994).
- [21] D. Munzar *et al.*, Solid State Commun. **112**, 365 (1999).
- [22] M.C. Schabel *et al.*, Phys. Rev. B **57**, 6090 (1998).